Turbulent Flow of Unstable Liquid-Liquid Dispersions: Drop Sizes and Velocity Distributions

J. P. WARD and J. G. KNUDSEN

Oregon State University, Corvallis, Oregon

Friction losses, velocity distributions, and drop size distributions were obtained for unstable liquid-liquid dispersions in turbulent flow. The friction losses and velocity profiles were used to determine effective viscosities which were correlated by the Einstein relation for dispersions in which $\mu_d/\mu_c \leqq 15$. When $\mu_d/\mu_c \approx 200$ the dispersion could not be considered as a single-phase fluid and exhibited non-Newtonian characteristics. Drop size distributions were obtained from photographs of the flowing dispersion. These drop size distributions provided information concerning drop breakup and coalescence in the circulation system. From drop size distribution and effective viscosity measurements a criterion was obtained to determine if a dispersion could be treated as a homogeneous single-phase fluid.

Previous studies (*1* to *5*) of unstable liquid-liquid dispersions in turbulent flow have been directed toward the determination of friction factors and heat transfer coefficients and the determination of suitable physical properties by which these quantities could be correlated. The fluids studied have been oil-in-water dispersions in which the discontinuous oil phase existed as fine droplets in the continuous water phase. The main variables investigated were flow rate and viscosity of the oil phase. For the most part, the dispersions have behaved as homogeneous Newtonian fluids.

There are certain maximum drop sizes, however, beyond which the dispersion will not behave as a homogeneous fluid or may have non-Newtonian properties. In previous studies no measurements of drop size or drop size distribution have been made, although one investigation (*1*) reported a criterion which could be used to determine if a dispersion could be treated as a single-phase fluid. The present investigation was undertaken to obtain information on the drop size and drop size distribution of liquid-liquid dispersions in turbulent flow. In addition, velocity distributions were measured for dispersions of highly viscous oils in order to extend the work of Faruqui and Knudsen (*4*).

A difficult aspect of the investigation was the development of a means of obtaining photographs of the dispersions so that drop sizes could be determined. Many techniques have been devised to photograph two-phase fluids. Kintner et al. (*6*) presented a review of the many photographic techniques which have been used in bubble and drop research. Most techniques are applicable to drops larger than 100 μ. Sleicher (*7*) and Brown and Govier (*8*) have photographed relatively large drops (0.2 to 0.8 cm.) present in a turbulent stream. Langlois et al. (*9*) and Trice and Rodger (*10*) used a light transmittance technique to obtain the average drop size of a dispersed oil phase in a mixer. This method is limited to drop sizes greater than about 50 μ (*11*).

The dispersion studied in the present work is unstable, relatively opaque except in extremely thin layers, and has drop sizes much less than 50 μ. Because of its unstable nature it had to be photographed in the test section under flow conditions.

BACKGROUND THEORY

This investigation concerns the behavior of small liquid droplets in a turbulent field. The breakup of liquid drops in a turbulent field has been considered by several investigators (*12* to *14*). Hinze (*14*) attempted to organize and classify the various types of deformation of droplets and flow patterns which result in drop breakup. For systems in which the effect of the dispersed phase viscosity is small he gives the result

$$\frac{\rho_c \sigma d_{\max}}{\mu_c^2} = C \left(\frac{\mu_c^5 \epsilon}{\rho_c \sigma^4} \right)^{-2/5} \tag{1}$$

which was of a form which could be fitted to data which Clay (*13*) had obtained.

Sleicher (*7*) investigated the maximum drop size in turbulent flow in a pipe and showed that it depended upon the -2.5 power of the velocity. He also determined from Clay's data that the maximum drop size depended on the same power of velocity and was not quite directly proportional to the interfacial tension. Sleicher noted that breakup occurred very close to the wall where turbulence was least isotropic and least homogeneous. Two types of breakup were observed: breakup of a drop into two equal parts (most frequent), and stripping of small droplets from large ones. Sleicher correlated his results within $\pm$ 35% by the equation

$$\frac{d_{\max} \rho_c U^2}{\sigma} \sqrt{\frac{\mu_c U}{\sigma}} = 38 \left[1 + 0.7 \left(\frac{\mu_d U}{\sigma} \right)^{0.7} \right] \tag{2}$$

Coalescence processes have been studied experimentally by Madden and Damerell (*15*) and theoretically by Haworth (*16*). The former found that frequency of coalescence in dilute (0.1 to 0.7 vol. %) dispersions varied as the square root of the volume fraction. Haworth proposed the following expression for coalescence frequency of droplets

$$\nu = \left(\frac{24 \phi d_c \overline{v^2}}{d_p^3} \right)^{1/2} \exp \left(\frac{3 w^{*2}}{4 \overline{v^2}} \right) \tag{3}$$

The variation of coalescence frequency with the square

root of the volume fraction in Equation (3) is in agreement with the results of Madden and Damerell.

The problem of predicting momentum and heat transfer for two-phase flow is considerably simplified if the systems can be handled by methods already developed for single-phase flow. By considering the equations of motion, Baron et al. (*1*) investigated the size of dispersed phase particle such that a single-phase equation might be applicable to the flow of the two-phase fluid. They concluded that the particle diameter must be small compared to the dimensions of the region of viscous flow. These workers chose as the dimension of the region of viscous flow the Kolmogoroff microscale of turbulence (*17*). Thus

$$d_p << l_k \tag{4}$$

where

$$l_k = \epsilon^{-1/4} (\mu/\rho)^{3/4} \tag{5}$$

They considered the ratio of inertia forces acting on the dispersed phase to the drag forces and arrived at the following criterion by which a dispersion could be considered to behave like a single-phase homogeneous fluid.

$$N_{Re_c} \left(\frac{d_p}{D}\right)^2 \left(\frac{\rho_d}{\rho_c}\right) \leq 1 \tag{6}$$

Application of Equation (6) to a liquid-liquid dispersion flowing in a 4-in. pipe at $N_{Re_c} = 10{,}000$ indicates that the drop diameter should be less than 1 mm. For water droplets suspended in a stream of air in a 3-in. pipe at $N_{Re_c} = 10^6$, the droplets must be less than 6 microns in diameter.

EXPERIMENTAL EQUIPMENT

A schematic flow diagram of the apparatus is shown in Figure 1. The dispersion, consisting of an organic and a water phase, was contained in a supply tank. A turbine pump circulated the dispersion from the bottom of the tank through an orifice, through one of two test sections, through a small heat exchanger, and back to the tank. One test section was equipped to measure friction losses, velocity profiles, and concentration profiles and the other contained the apparatus for photographing the flowing dispersion. The two test sections were identical: 1-in. O.D., 0.830-in. I.D. copper tube 9½ ft. long. The flow was switched between the test sections by a solenoid valve located at the end of each section. Velocity profiles were measured with a calibrated impact probe made from 0.049-in. O.D. and 0.033-in. I.D. stainless steel hypodermic tubing. The measuring devices, either Pitot tube, or photographic window, were located 8½ ft. from the entrance of the test sections. Pressure taps were located 2½ and 8½ ft. from the entrance of the test section.

TABLE 1. PROPERTIES OF OILS USED AS DISPERSED PHASES

Temperature, °F,	Density, lb./cu. ft.	Viscosity, centipoise	Interfacial tension, dyne/cm.
62	49.05, 53.93, 55.32*	1.06, 18.2, 261	
68	48.92, 54.25, 55.22	1.01, 15.6, 214	
74	48.73, 53.62, 55.13	0.95, 13.0, 162	
			49, 52, 48

* Shellsolv, light oil, and heavy oil, respectively.

The organic phases were a commercial petroleum solvent (Shellsolv 360) and two clear, highly refined oils (Standard of California white oil No. 1 and white oil heavy). The physical properties of these liquids are given in Table 1.

The arrangement for photographing the flowing dispersion is shown diagramatically in Figure 2. The window through which the pictures were taken was made by milling off part of the copper tube wall until an opening 3 in. by ¼ in. was formed. The wall was then replaced by a thin glass plate (microscope slide glass, 1 mm. thick) which was set in a Plexiglas block 3 in. by 1⅝ in. by ¼ in. A ¾-in. diameter hole in the center of this block allowed the objective lens of the microscope to be brought up to the outside of the glass window. The glass had to be sufficiently thin to allow the plane of focus of the microscope to fall inside the pipe.

The photographs were taken with an American Optical Company Microstar Trinocular microscope equipped with a 35-mm. photomicrographic camera (model 635). The image could be focused while looking through the binocular eyepiece and then transferred to the camera by simply moving a prism. Most of the pictures were taken with a 10-power objective lens, although for a few runs this gave too large a depth of focus and it was necessary to use the 20-power objective. Since this brought the plane of focus much closer to the wall it was used only when absolutely essential. An electronic stroboscope provided the short flash duration necessary to stop the motion of the rapidly flowing droplets.

This photographic arrangement was first developed on a smaller and much simpler flow system than shown in Figure 1. Scotchlite glass beads were used in conjunction with this small-scale system to test the validity of the photographic technique. The beads ranged in diameter from 5 to 115 microns with an average diameter of 43 microns; thus the test was conducted with spheres of about the same size as the droplets in a typical liquid-liquid dispersion.

In one experiment, the window arrangement shown in Figure 2 was replaced with a window similar to that used by Scott, Hayes, and Holland (*18*), which consisted of a rectangular converging-diverging section of pipe with glass windows placed on opposing sides of the broadened pipe walls (Figure 3). The cross-sectional area of this unit is constant and equal to that of the test section tube to which it

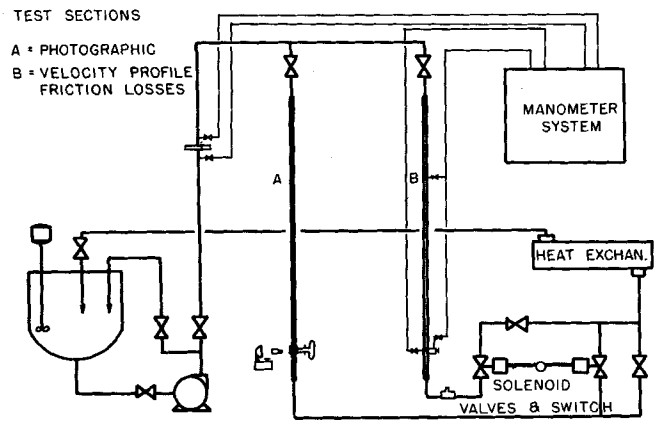

Fig. 1. Flow diagram of experimental equipment.

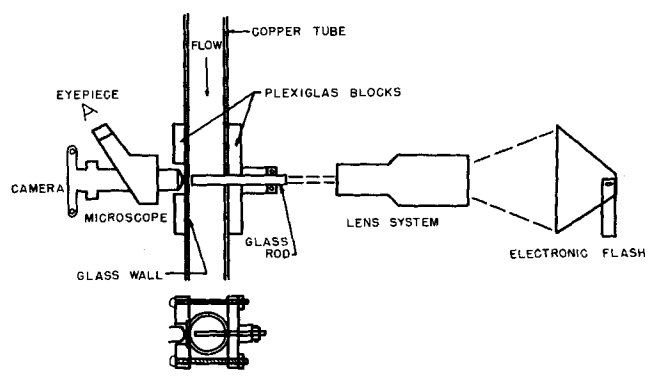

Fig. 2. Arrangement for photographing flowing dispersions.

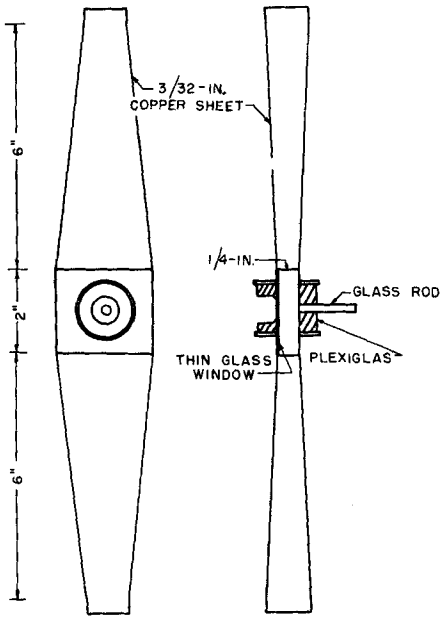

Fig. 3. Converging-diverging window section.

is connected. The purpose of this experiment was to determine if the glass rod arrangement shown in Figure 2 caused undue breakup of the droplets.

Table 2. Summary of Experimental Program

Run*	Observations Type	No.	Mass flow rate, lb./hr.	Dispersed phase Concentration vol. fraction
W	Pressure loss	20	0.560-3.110	0
S01	Photographic	—	4.07	0.01
S05	Photographic	—	1.20, 1.96, 3.02, 4.18	0.05
S10	Photographic	—	4.04	0.10
S15	Photographic	—	3.88	0.15
L01	Photographic	—	3.86	0.01
L05	Photographic	—	2.56	0.05
L10	Pressure loss	14	1.03-3.98	0.085
	Velocity profile	3	1.25, 2.55, 3.98	
	Photographic	—	1.25, 2.55, 3.98	
L20	Pressure loss	16	0.85-4.23	0.162
	Velocity profile	3	1.12, 2.51, 3.68	
	Photographic	—	1.12, 2.51, 3.68	
L35	Pressure loss	16	0.74-3.98	0.33
	Velocity profile	3	1.00, 2.38, 3.72	
	Photographic	—	1.00, 2.38, 3.72	
L50	Pressure loss	14	0.94-3.98	0.47
	Velocity profile	3	1.09, 2.24, 3.70	
	Photographic	—	1.09, 3.57	
H01	Photographic	—	3.95	0.01
H05	Pressure loss	7	1.65-4.00	0.05
	Photographic	—	3.85	
H10	Pressure loss	13	1.00-3.80	0.10
	Velocity profile	2	1.50, 3.80	
	Photographic	—	3.63	
H20	Pressure loss	11	1.03-3.62	0.20
	Velocity profile	2	1.60-3.70	
	Photographic	—	3.62	
H27	Pressure loss	13	0.99-4.00	0.27
	Velocity profile	2	1.56, 3.70	
H35	Photographic	—	3.70	0.35

* W = water, S = Shellsolv, L = light oil, H = heavy oil.

EXPERIMENTAL PROGRAM

Oil-in-water dispersions of desired composition were made by charging known quantities of oil and tap water to the system. A run was always started with fresh oil and water and only after the system had been thoroughly flushed after the preceding run. Before beginning the experimental program the system was thoroughly flushed with cleaning solvent, followed by hot disodium phosphate, followed by a thorough flushing with water. At the completion of a run the dispersion was allowed to separate in the tank and the water phase including the interface was removed as waste. The remaining clear oil phase was reused.

In some runs photographs were taken periodically to determine when the drop size distribution became steady. This equilibrium was normally established after 3 hr. of circulation and agitation. All equilibrium drop sizes were determined after 5 hr. of circulation to ensure that equilibrium had been established.

After the required number of photographs had been obtained for each run, velocity distributions and friction losses were determined. In all runs system temperature was controlled at 68 ± 2°F. by adjusting cooling water rate to the heat exchanger.

A summary of experimental data is shown in Table 2. Complete data are tabulated elsewhere (*19*).

DISCUSSION OF RESULTS

Pressure Losses and Velocity Profiles

The purpose of the pressure loss and velocity profile investigations was to determine the effective viscosities of the light and heavy oil dispersions. The Shellsolv dispersions had previously been studied by Cengel et al. (*2*) and Faruqui and Knudsen (*4*).

To determine an effective viscosity of the dispersion from pressure loss measurements use is made of the equation

$$\Delta p_f = K\mu_e^{0.25}W^{1.75} \tag{7}$$

where K is a dimensional coefficient determined from length and diameter of the test section and density of the flowing fluid. Equation (7) is based on the Blasius friction factor–Reynolds number relationship and the assumption that the two-phase dispersion behaves as a homogeneous Newtonian fluid. A logarithmic plot of Δp_f vs. W should give a straight line of slope 1.75 and this result was obtained on all pressure loss data except for heavy oil dispersions at low flow rates.

Again by assuming a homogeneous Newtonian fluid, the velocity distribution data were fitted to a logarithmic velocity distribution equation

$$u^+ = A \log y^+ + B \tag{8}$$

where

$$y^+ = yu^*\rho_e/\mu_e$$

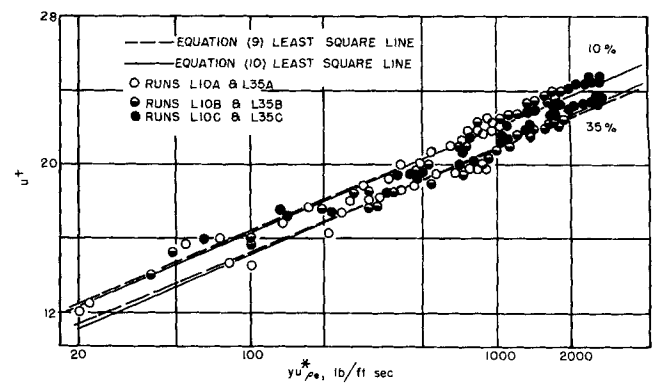

Fig. 4. Velocity profiles for 10 and 35% light oil dispersions.

Table 3. Relative Fluidities (at 68°F.) of Oil-in-Water Dispersions

Volume fraction dispersed phase	Relative fluidity, μ_c/μ_e: From pressure loss measurements Equation (7)	From velocity-profile measurements Equation (10)	Predicted from Equation (11)
Light oil:			
0.085	0.740	0.782	0.809
0.162	0.671	0.690	0.667
0.33	0.440	0.478	0.448
0.47	0.302	0.311	0.309
Heavy oil:			
0.05	0.730	—	0.882
0.10	0.752	—	0.779
0.20	0.752	—	0.607
0.27	0.885	—	0.509

and hence

$$y^+\mu_e = yu^*\rho_e$$

The quantity $yu^*\rho_e$ may be calculated from experimental data.

If the viscosity is constant, Equation (8) may be expressed as

$$u^+ = A \log (yu^*\rho_e) + B' \qquad (9)$$

where

$$B' = B - A \log \mu_e$$

A plot of u^+ vs. the dimensional quantity $yu^*\rho_e$ [lb./(ft.)(sec.)] is shown in Figure 4 for the 10 and 35% light oil dispersions. The broken lines represent a least square analysis of the data according to Equation (9).

For the light oil dispersions the value of A decreased from 5.71 for the 10% dispersion to 5.27 for 50% dispersion, while B' decreased from 5.01 to 3.94 over the same concentration range. The results for the heavy oil dispersions did not show this consistent trend and were not as reproducible as were the data for the light oil dispersions.

Since the value of A for the light oil dispersions was close to the value of 5.75 (the usual value for single-phase Newtonian fluids), the data for these dispersions were analyzed by the method of least squares according to the following equation:

$$u^+ = 5.75 \log (yu^*\rho_e) + B'' \qquad (10)$$

where

$$B'' = B - 5.75 \log \mu_e$$

The solid lines in Figure 4 represent Equation (10). From the values of B'', values of the dispersion viscosity μ_e are calculated by assuming $B = 5.5$ (the value of B for Newtonian single-phase fluids). A similar analysis for the heavy oil dispersions produced widely varying viscosities.

Table 3 shows calculated viscosities expressed as relative fluidities with respect to the fluidity of the continuous phase. The last column of Table 3 shows the relative fluidity calculated from the equation

$$(\mu_c/\mu_e) = e^{-2.5\phi} \qquad (11)$$

which was derived by Einstein (20) for suspensions of uniform solid spheres and for very low volume concentrations.

For the light oil dispersions good agreement is obtained between Equations (7) and (10). It is interesting to note that Einstein's equation, which was derived for low concentrations of uniform spheres, applies to well-dispersed light oil dispersions up to a volume fraction 0.5. These results also agree well with the results for Shellsolv dispersions reported by Faruqui and Knudsen (4). The viscosity of the heavy oil dispersions is nearly constant and even shows a tendency to decrease at higher concentrations. This phenomenon is discussed in more detail in a subsequent section on the basis of drop size and distribution.

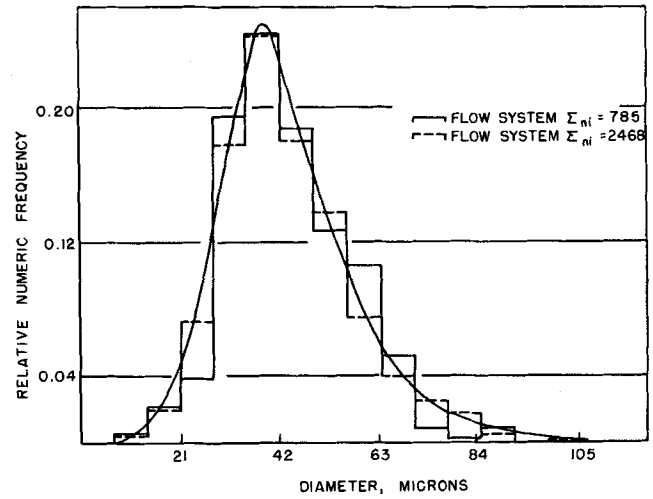

Fig. 5. Glass bead distribution curves.

Evaluation of the Photographic Method

A small-scale system was constructed in which glass beads could be circulated. This system was used to develop the window and glass rod arrangement shown in Figure 2.

Photographs of a suspension of glass beads of known size distribution were obtained under flowing conditions. The size distribution was determined from the photographs and compared with a size distribution obtained by counting a sample viewed with a microscope. The results are shown in Figure 5. Fairly large discrepancies in frequency occur at high diameters but these tend to cancel each other and the frequency curve for the flow system is very close to that obtained by counting stationary beads.

The photographic arrangement was not completely ideal because of the presence of the glass rod in the flow-

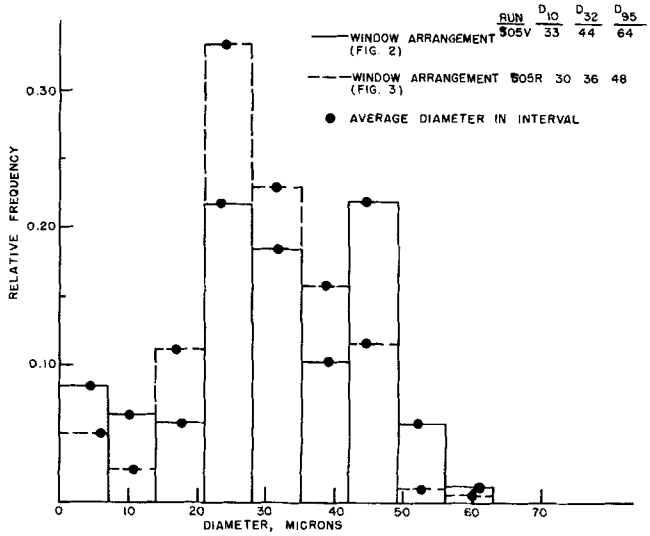

Fig. 6. Comparison of two photographic arrangements (see Figures 2 and 3).

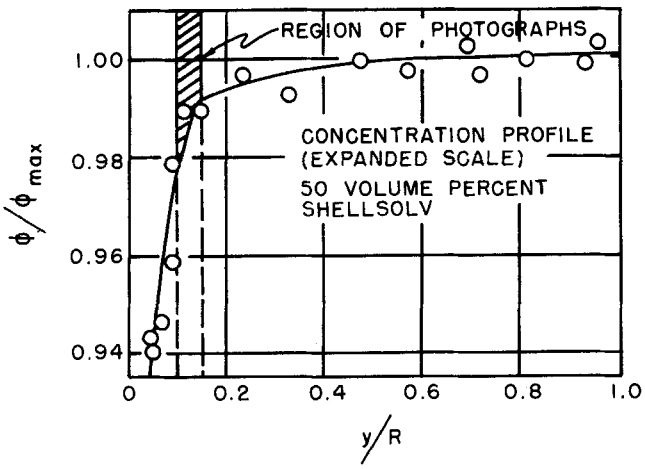

Fig. 7. Concentration profile for 50% Shellsolv dispersion.

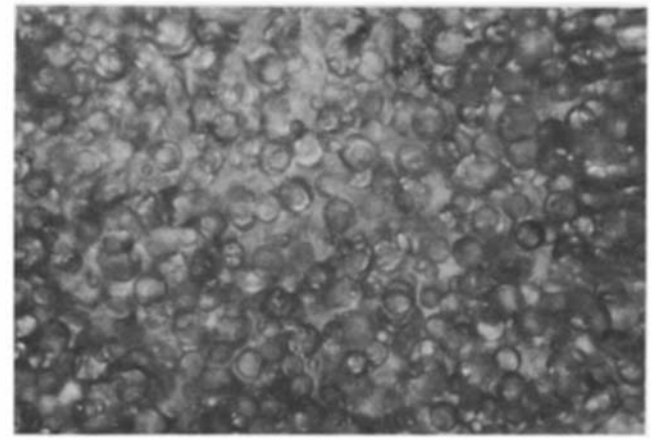

Fig. 8a. Run S20A, Roll 86, $N_{Re} = 1.9 \times 10^4$, $t = 300$ min.

ing stream. However, in over 90% of the more than 1,000 photographs taken during this study, the droplets appeared spherical and only showed some deformation at the high concentrations. Thus it was concluded that the effect of the glass rod on the measured drop sizes and distributions was negligible. In an attempt to obtain data to verify the above conclusion, a dispersion of 50% Shellsolv was photographed with the usual glass rod system and also with the special window section shown in Figure 3. In this latter arrangement the glass rod did not project into the stream. The distribution for both arrangements is shown in Figure 6. The glass rod system shows somewhat higher frequency of droplets in the 0- to 14-micron range. This indicates some probable breakup due to the glass rod. On the average the glass rod arrangement shows higher average diameters than the converging-diverging section, a result which is opposite to what would have been obtained if excessive breakup were occurring in the vicinity of the glass rod. In addition, it was found that the arrangement in Figure 3 could only be used for dispersions containing no more than 5% dispersed phase. Hence, the glass rod arrangement, even though it caused some disturbance in the flow, was useful over a wider range of experimental conditions.

Since the plane of focus, that is, the plane being photographed, was within what would be the turbulent core in the unobstructed pipe, it was assumed that the drop size distribution obtained was representative of that over the whole turbulent core. However, a radial variation of drop size quite probably exists. Such a radial drop size variation might be reflected by a concentration variation; hence a concentration profile for the dispersion containing 50% Shellsolv was obtained as shown in Figure 7. The concentration is nearly constant over the region $0.15 < y/R < 1.0$ and then decreases rapidly at values of $y/R < 0.15$. The photographs depicted the region $0.10 < y/R < 0.15$ where the concentration was 97 to 99% of the concentration in the central portion of the tube. Therefore, the photographs very nearly depict the conditions in the turbulent core of the tube. The concentration profile shown in Figure 7 agrees qualitatively with the negative radial migration of deformable drops in laminar flow observed by Goldsmith and Mason (*21*).

Drop Size and Drop Size Distribution

Over 1,000 photographs of dispersions were obtained. Typical photographs are shown in Figures 8*a*, 8*b*, 8*c*, and 8*d*. One 20-frame roll of 35-mm. film was used for each run. The diameters of the well-defined droplets appearing on the photographs were measured and these were used to calculate a number of characteristic average diameters, namely, D_{10}, D_{32}, and D_{95}, which are defined as follows:

$$D_{10} = \frac{\sum_{j=1}^{n} d_j}{n}$$

$$D_{32} = \frac{\sum_{j=1}^{n} d_j^3}{\sum_{j=1}^{n} d_j^2}$$

D_{95} = diameter of particles below which 95% of the volume of the dispersed phase is contained (95th volumetric percentile).

The number of droplets counted in determining the distribution was between 300 and 500 for a majority of the runs.

The complicated nature of the flow system prevents drawing definite conclusions concerning the drop size distribution data and its relationship to fluid mechanical behavior. The analysis is further restricted by the fact that photographs were obtained at only one location in the system.

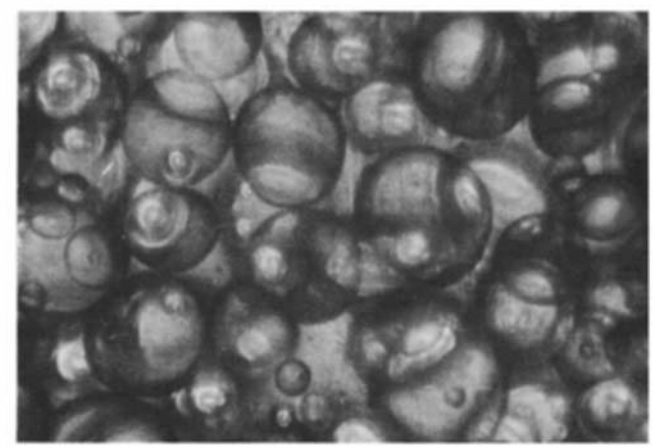

Fig. 8b. Run S50B, Roll 88, $N_{Re} = 1.7 \times 10^4$, $t = 300$ min.

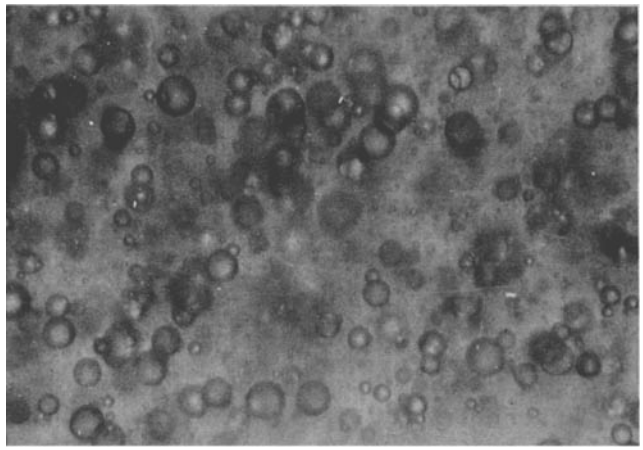

Fig. 8c. Run LO5A, Roll 42, $N_{Re} = 1.2 \times 10^4$, $t = 25$ min.

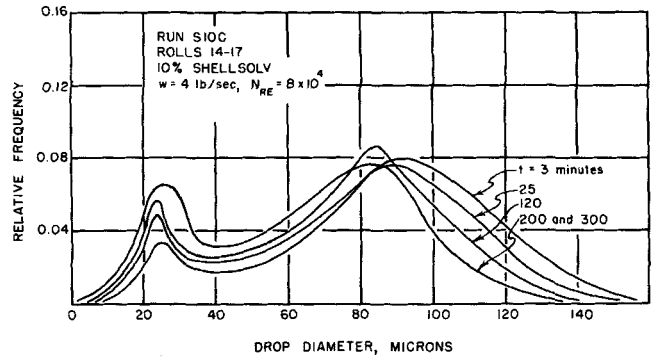

Fig. 9. Drop size distribution as a function of time.

There are two possibilities with respect to droplet breakup and coalescence. In one, droplet breakup predominates in regions of high shear such as in the pump, in the mixing tank, and at various points of disturbance throughout the system. Coalescence would predominate in regions of low shear and hence an equilibrium would be attained throughout the system. However, the state of dispersion at different locations would be different. The second possibility is that breakup and coalescence occur at equal rates at all points in the system so that the state of equilibrium is nearly the same everywhere. Whichever possibility exists it seems reasonable to assume that the distribution obtained from the photographs nearly approximated what was flowing in the test section, since at the lowest flow rate the residence time in the test section was only 2 sec. Hence, the fluid mechanical behavior observed is probably representative of the dispersion photographed.

Figure 9 shows the drop size distributions for a 10% Shellsolv dispersion as a function of time. These were characteristics of all Shellsolv dispersions with more than 5 vol. % dispersed phase. The curve is characterized by two peaks, one in the vicinity of 25 microns and one in the vicinity of 70 microns. As circulation proceeds, the position of the peaks remains relatively constant with respect to diameter but the relative frequency changes, decreasing for the peak at the higher diameter and increasing for the peak at the lower diameter.

The shape of the distribution curve is a function of the concentration and of the physical properties of the two liquids making up the dispersion. Figure 10 shows the effect of concentration when compared with Figure 9. At early stages, the curve is similar to those shown in Figure 9; however, the peak at the higher diameter disappears as equilibrium is approached in the system. This is a possible indication that the two peaks in Figure 9 are indicative of breakup (the lower diameter peak) and coalescence (the higher diameter peak). In Figure 10 the absence of the higher diameter peak indicates that coalescence may become negligible at low concentrations.

Figure 11 compares the characteristic drop size distribution of the Shellsolv, light oil, and heavy oil dispersions at the same flow rate and same concentration. The differences in the curves are therefore indicative of the effect of dispersed phase viscosity, since the interfacial tension of all three oils in water was nearly the same. The light oil showed a characteristic high peak in the range between 50 and 100 microns, depending on concentration. The largest drops observed in the light oil dispersion were up to twice the diameter of those in the Shellsolv dispersions. The heavy oil dispersions showed only a high peak in the 0- to 7-micron range. However, extremely large drops

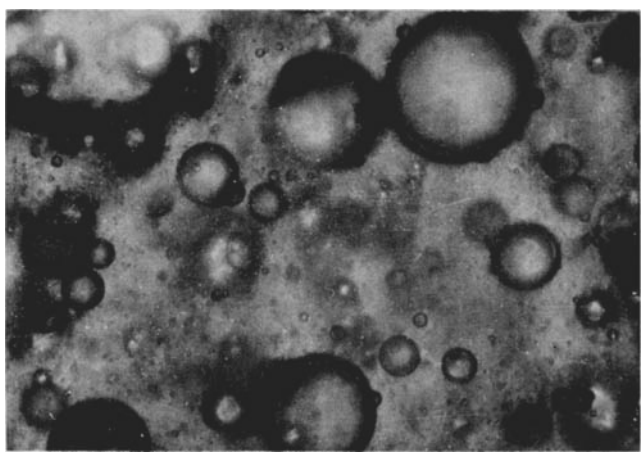

Fig. 8d. Run H10A, Roll 75, $N_{Re} = 1.2 \times 10^4$, $t = 600$ min.

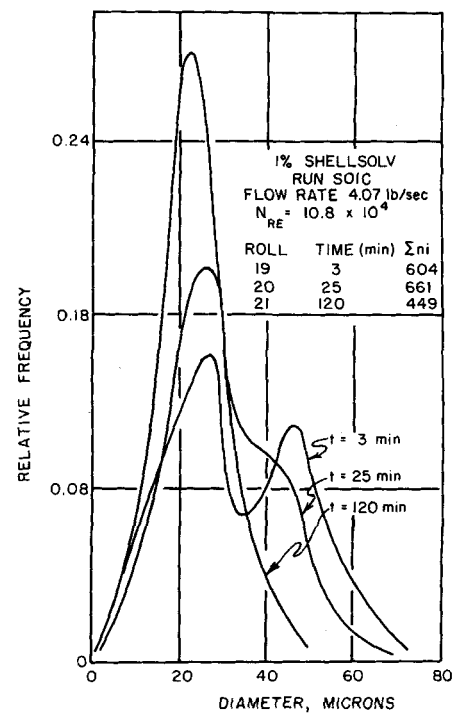

Fig. 10. Drop size distribution as a function of time.

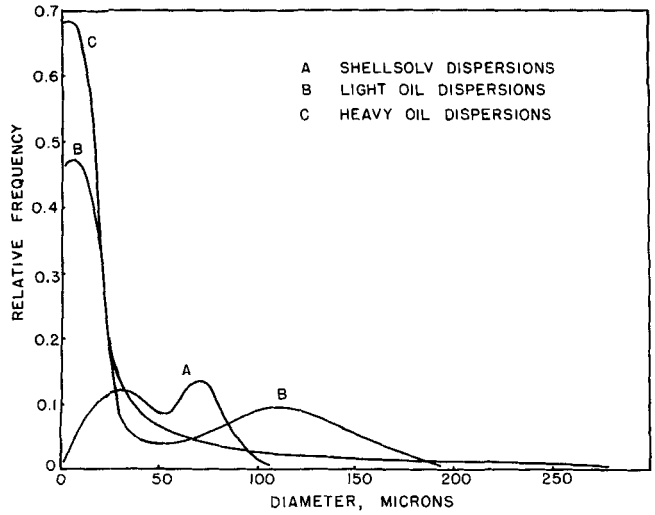

Fig. 11. Comparison of drop size distribution for different dispersed phases.

were observed (up to 800 microns). Although these large drops had a low numeric frequency, they contained most of the volume of the dispersed phase present.

Figure 12 shows the effect of dispersed phase concentration on droplet diameter. This diameter varies approximately as the 0.4 power of the dispersed phase concentration. The heavy oil dispersions have considerably higher average diameters than the Shellsolv and light oil dispersion.

Two different types of drop breakup have been proposed by Clay (*13*) and have been observed experimentally by Sleicher (*7*). In one type the drop is broken into approximately two equal drops, while in the second type a local region of reduced pressure produces a small protuberance which breaks off in the form of a small drop, leaving the original drops only very slightly changed in diameter. Sleicher (*7*) observed both types in a turbulent field in systems where the viscosities of the two phases were nearly equal. However, the first type occurred most frequently.

It is possible that both types of breakup occur in the dynamic system being studied. However, if the high-diameter peak represents the source of those droplets in the low diameter peak, then for the type of breakup into equal parts by volume the low peak should occur at a diameter of about eight tenths of the diameter at the high peak. The positions of the two peaks suggest unequal breakup of the droplets. As an approximation the positions of the Shellsolv peaks suggest that the drop formed at breakup is about 4% of the volume of the parent drop. (This is based on a 25- and 75-micron position of the low and high peaks, respectively.) Likewise, for the light oil, the drop formed at breakup is approximately 0.03% of the volume of the parent drop (based on 5- and 75-micron peaks).

This strongly suggests that the breakup is predominantly of the type where a drop breaks off a much larger drop, leaving it virtually unchanged. However, this is an oversimplified picture and other phenomena, such as mechanism of coalescence and localized high rates of breakup and coalescence in the system, no doubt influence the position of the peaks in the drop distribution curves. The question of the character of the drop distribution at every location in the system is unresolved but some experiments were made which qualitatively show the effect of the pump in the system.

Possibly the high-speed turbine pump impellers were a location of high rate of breakup. The pump output was approximately constant and the flow rate in the test section was controlled by varying the amount returning to the mixing tank through a short bypass line. In one experiment, the flow system was modified so that dispersion flowed directly from the pump through about 2 ft. of tubing to the photographic test section and thence directly back to the tank. Hence, the dispersion being photographed was nearly representative of that leaving the pump for all other experiments. The results are shown in Figure 13. The point corresponding to zero circulation rate through the test section represents the dispersion coming directly from the pump. The dispersions at flow rates between 1 and 4 lb./sec. flowed through about 12 ft. of 1¼ pipe and through the 8½-ft. long test section. The diameter is lower for the dispersion coming directly from the pump than for low flow rates through the test section, indicating coalescence was taking place in the 20 ft. of pipeline between the pump and photographic arrangement. At high flow rates, the diameter in the test section is nearly the same as that for the dispersion leav-

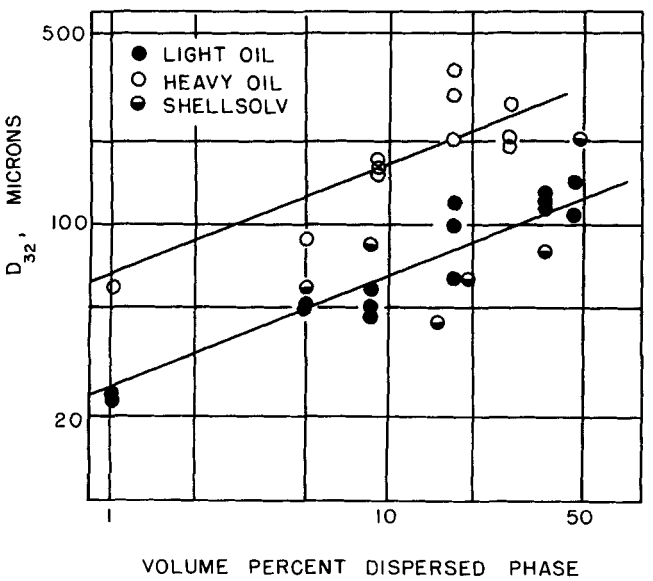

Fig. 12. Variation of drop size with concentration.

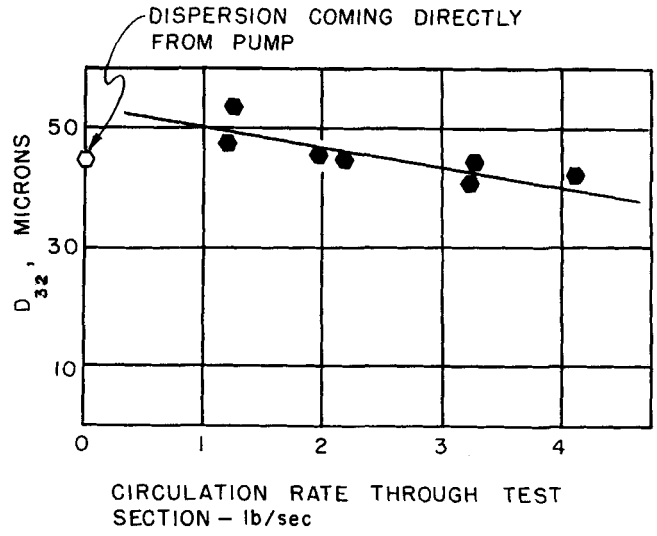

Fig. 13. Effect of pump on drop breakup for 5 vol. % Shellsolv dispersion.

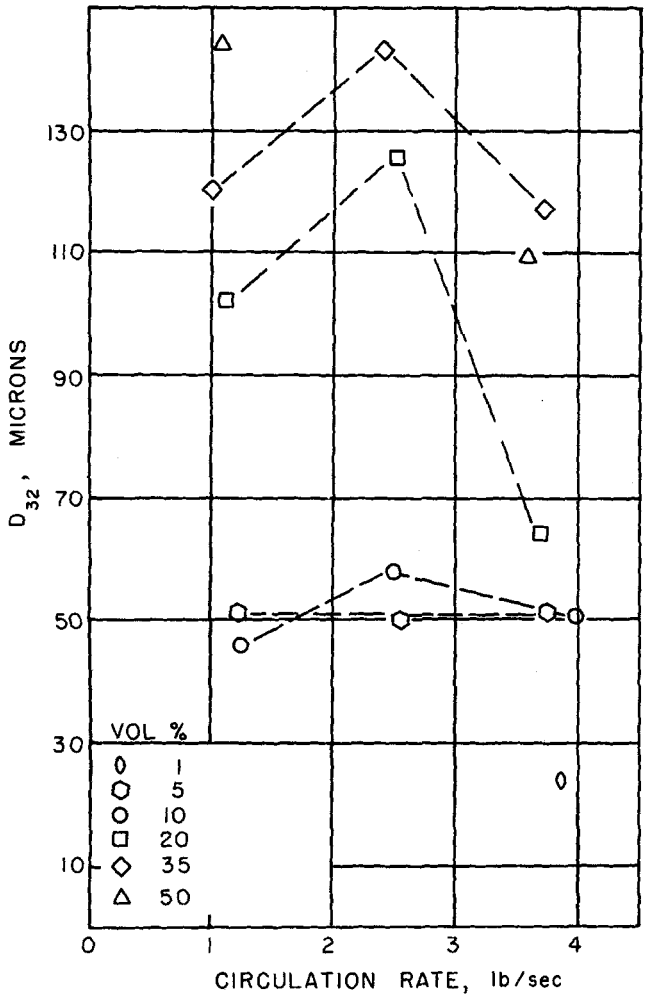

Fig. 14. Droplet diameter for light oil dispersions.

ing the pump. This would indicate that the processes of breakup and coalescence in the intervening pipeline were essentially in equilibrium at these higher flow rates.

Any high rates of breakup occurring in the piping system are probably at flow restrictions. In straight pipe sections, coalescence is probably the dominant phenomenon. This reasoning is based upon Sleicher's empirical equation for maximum stable drop size in turbulent flow [Equation (2)]. Appreciable breakup would occur in straight pipe sections if drops were of this size or greater. Equation (2) indicates that maximum drop diameters at 4 lb./min. flow for the Shellsolv, light oil, and heavy oil are, respectively, 250, 350, and 1,400 microns. These increase to 6,000, 7,000, and 18,000 microns at a flow rate of 1 lb./sec. Therefore it appears that drop sizes in the system are largely dependent upon the action of the pump with breakup also occurring at flow restrictions, this being nearly balanced by coalescence.

Figure 14 shows the effect of both circulation rate and dispersed phase concentration on the diameter for the light oil dispersions. For a given concentration the largest diameters occur at the flow rates midway between 1 and 4 lb./sec. with the exception that at 5% concentration diameter is essentially independent of flow rate. Sleicher's (7) results show that drop breakup depends strongly on velocity (−2.5 power). This presumably would be applicable in flow restrictions as well as in straight tubes. This would explain smaller drop sizes at high flow rates. The higher diameters in the midrange of flow rates would indicate coalescence effects. This would agree with the theory proposed by Haworth (*16*) [Equation (3)], which predicts an increase in coalescence frequency both with increasing velocity and concentration. At the higher flow rates, the strong effect of velocity on breakup evidently becomes predominant over the coalescence thus causing the decrease in average diameter.

For the heavy oil dispersions smaller diameters were observed at the 4 lb./min. flow rate than at the 1 lb./min. Intermediate flow rates were not studied.

Single-Phase Criterion

One of the purposes of this study was to compare the momentum transfer of the dispersions with the drop sizes of the dispersed phase. Baron et al. (*1*) presented Equation (6) as a criterion by which two-phase dispersions could be treated as single-phase homogeneous fluids. This criterion was based upon the requirement that the dispersed phase particles should be smaller than the Kolmogoroff microscale of turbulence l_k. In the present study it is postulated that the following criterion holds

$$N_{Re}\left(\frac{d_p}{D}\right)^2 \frac{\rho_d}{\rho_e} \leq N \qquad (12)$$

where N is a constant to be determined.

It is necessary to choose an appropriate particle diameter for the above relationship and it would be desirable to choose a quantity which is not strongly dependent upon the drop size distribution. The maximum drop size or the 95th volumetric percentile (D_{95}) is subject to large statistical variations, particularly for small samples. The diameter D_{32} best represents the average size of the largest drops and is only slightly influenced by the size and number of small drops.

In Figure 15 D_{32} is plotted vs. Reynolds number (based on effective viscosity). The solid line represents Equation (12) when $N = 2$. The broken line is a plot of the Kolmogoroff microscale of turbulence calculated from

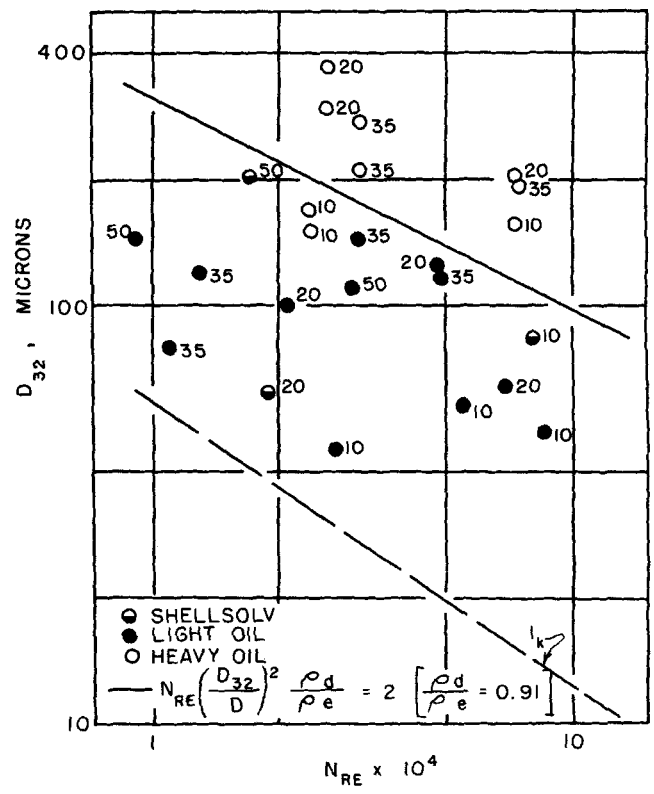

Fig. 15. Drop diameter as a function of Reynolds number.

Equation (5). The Shellsolv and light oil dispersions have been found to behave similar to homogeneous Newtonian fluids and data for these dispersions fall below the solid line. The heavy oil dispersions fall above the solid line and did not behave the same as the Shellsolv and light oil dispersions. The apparent viscosity of the heavy oil dispersions was nearly independent of concentration and the velocity profiles indicated non-Newtonian characteristics.

The value of D_{32} of the heavy oil dispersions is of a magnitude that the dispersion cannot be treated as a single-phase fluid. The fact that the effective viscosity of the heavy oil dispersions (from friction factor measurements) was nearly independent of concentration can be explained to some extent from the drop size distribution. There are many small droplets. Approximately 70% of the droplets are less than 30 microns but these only account for 0.3% of the volume of the dispersed phase. Only 5% of the drops are in the 100- to 300-micron range but these account for 85% of the volume of the dispersed phase. The heavy oil dispersions are multiple dispersions of a few large drops and many small drops. Doubling the dispersed phase concentration will effectively cause a 25% increase in the diameter of the large drops if their number remains constant. Thus the 10, 20, and 27% heavy oil dispersions are similar in nature and cannot be treated as homogeneous Newtonian fluids.

It is concluded that criterion

$$N_{Re}\left(\frac{D_{32}}{D}\right)^2 \frac{\rho_d}{\rho_e} \leq 2 \qquad (13)$$

provides a possible means for determining if oil-in-water dispersions behave as homogeneous Newtonian fluids. This conclusion is strictly limited to the three oil-in-water systems studied in the present investigation. This criterion is within the order of magnitude of that derived theoretically by Baron et al. (*1*).

CONCLUSIONS

This has been a study of friction losses, velocity profiles, and drop size distributions of liquid-liquid dispersions in turbulent flow. The study of drop size distributions provided qualitative information concerning the breakup and coalescence processes in the flow system.

For the systems studied a criterion for determining if a liquid-liquid dispersion behaves as a homogeneous Newtonian fluid is proposed in Equation (13).

Effective viscosities of light oil dispersions following the criterion of Equation (13) could be suitably predicted by Einstein's equation [Equation (11)]. The results agree with those obtained by Faruqui and Knudsen (*4*) on Shellsolv dispersions. The effective viscosity was determined both from friction factors and velocity profiles, and each method gave comparable values.

Heavy oil dispersions showed an anomalous behavior, which was explained on the basis of their drop size distribution.

The most frequent drop sizes in the Shellsolv dispersions were 25 and 50 to 70 microns. As dispersed phase viscosity increased, the drop size distribution indicated a preponderance of very small droplets and few large drops, these large drops constituting most of the volume of the dispersed phase in the dispersion.

The turbine circulating pump appears to be a location of high rate of drop breakup in the system. Coalescence probably is predominant at locations of low shear rates. In the equilibrium condition the average drop size increases with concentration and first increases then decreases with flow rate. The latter effect of flow rate represents the relative predominance of the breakup and coalescence processes as affected by velocity.

ACKNOWLEDGMENT

The authors express appreciation to the National Science Foundation for a research grant (No. GP-2249), which provided support for the research described herein. Appreciation is also expressed to Standard Oil Company of California for supplying the light and heavy oils used as dispersed phases.

NOTATION

A, B = constants in Equation (8)
B', B'' = constants in Equations (9) and (10), respectively
C = constant in Equation (1)
D = tube diameter, L
D_{10} = arithmetic average diameter
D_{32} = mean diameter
D_{95} = ninety-fifth volumetric percentile, L
d_c = collision diameter
$d_{\max}$ = maximum stable drop size
d_j = diameter of j^{th} drop
d_p = particle diameter, L
K = constant in Equation (7), $1/mL^{.75}$
L = length
l_k = Kolmogoroff microscale of turbulence, L
m = mass
N = empirical constant in Equation (12)
n_i = number of drops counted in each diameter interval
Σn_i = total number of drops counted
Δp_f = pressure loss due to friction, m/Lt^2
R = tube radius, L
N_{Re} = Reynolds number based on effective viscosity of dispersion
N_{Re_c} = Reynolds number based on viscosity of continuous phase
t = time
U = average velocity, L/t
u = point velocity, L/t
u^+ = dimensionless velocity, u/u^*
u^* = friction velocity, L/t
$\overline{v^2}$ = mean square of the turbulent velocity fluctuation, L^2/t^2
w = mass flow rate, m/t
w^* = collision velocity, L/t
y = distance from tube wall, L
y^+ = dimensionless distance, $yu^*\rho/\mu$

Greek Letters

ϵ = energy dissipation in turbulent flow, L^2t^3
ν = frequency of coalescence, t^{-1}
μ_c = viscosity of continuous phase
μ_d = viscosity of dispersed phase
μ_e = effective viscosity of dispersion, m/Lt
ϕ = volume fraction of dispersed phase
$\phi_{\max}$ = volume fraction of dispersed phase at the tube axis
ρ_c = density of continuous phase
ρ_d = density of dispersed phase
ρ_e = density of dispersion, m/L^3
σ = interfacial tension, m/t^2

LITERATURE CITED

1. Baron, Thomas, C. S. Sterling, and A. P. Schueler, *Proc. Midwest Conf. Fluid Mech.*, 3, 103 (1953).
2. Cengel, J. A., M.S. thesis, Oregon State Coll., Corvallis (1959).
3. ———, A. A. Faruqui, J. W. Finnigan, C. H. Wright, and J. G. Knudsen, *A.I.Ch.E. J.*, 8, 335 (1962).

4. Faruqui, A. A., and J. G. Knudsen, *Chem. Eng. Sci.*, 17, 897 (1962).
5. Legan, R. W., M.S. thesis, Oregon State Univ., Corvallis (1965).
6. Kintner, R. C., et al., *Can. J. Chem. Eng.*, 39, 235 (1961).
7. Sleicher, C. A., Jr., *A.I.Ch.E. J.*, 8, 471 (1962).
8. Brown, R. A. S., and G. W. Govier, *Can. J. Chem. Eng.*, 39, 159 (1961).
9. Langlois, G. E., J. E. Gullberg, and Theodore Vermeulen, *Rev. Sci. Inst.*, 25, 360 (1954).
10. Trice, V. G., Jr., and W. A. Rodger, *A.I.Ch.E. J.*, 2, 205 (1956).
11. Rodger, W. A., V. G. Trice, and J. H. Rushton, *Chem. Eng. Progr.*, 52, 515 (1956).
12. Taylor, G. I., *Proc. Roy. Soc. (London)*, 138A, 41 (1932).
13. Clay, P. H., *Kon. Ned. Akad. Wetenschap.*, 43, 852, 979 (1940).
14. Hinze, J. O., *A.I.Ch.E. J.*, 1, 289 (1955).
15. Madden, A. J., and G. L. Damerall, *ibid.*, 8, 233 (1962).
16. Haworth, W. J., *Chem. Eng. Sci.*, 19, 33 (1964).
17. Kolmogoroff, A. M., *Compt. Rend. Acad. Sci. USSR*, 30, 301 (1941); 31, 538 (1941).
18. Scott, L. S., W. B. Hayes III, and C. D. Holland, *A.I.Ch.E. J.*, 4, 346 (1958).
19. Ward, J. P., Ph.D. thesis, Oregon State Univ., Corvallis (1964).
20. Einstein, Albert, *Ann. Phys.*, 19, 289 (1906).
21. Goldsmith, H. L., and S. G. Mason, *J. Colloid. Sci.*, 17, 448 (1962).

Manuscript received February 9, 1966; revision received August 15, 1966; paper accepted August 15, 1966.

Penetration Theory for Diffusion Accompanied by a Reversible Chemical Reaction with Generalized Kinetics

R. M. SECOR and J. A. BEUTLER

E. I. du Pont de Nemours and Company, Inc., Wilmington, Delaware

The penetration theory equations representing diffusion with a generalized, reversible chemical reaction of the form $\gamma_A A + \gamma_B B \rightleftharpoons \gamma_M M + \gamma_N N$ are solved by a finite-difference method. Many solutions are presented in graphical form. Approximate solutions to several limiting cases are obtained analytically by means of a steady state representation and are useful for estimating results of the solution to the penetration theory equations.

Since its inception, the penetration theory of Higbie (*14*) has been applied widely to unsteady state diffusional processes. The Higbie model has been particularly useful for solving many problems involving diffusion with chemical reaction. In most cases, interest has been directed toward diffusion of one reactant into a semi-infinite medium containing a second reactant that depletes the first according to some known kinetic mechanism. Obtaining an expression for the rate of diffusion of the first reactant through the boundary of the semi-infinite medium in general requires the solution of a set of simultaneous partial differential equations or in some cases a single such equation, with appropriate boundary conditions. Restrictions of various kinds have been placed on the physical problem in order to facilitate solution of these equations. Solutions to the penetration theory equations have been obtained for diffusion with:

J. A. Beutler is with General Electric Company, Schenectady, New York.